Design of three-mirror illumination system with free-form fly's eye for extreme ultraviolet lithography

Qiuli Mei and Yanqiu Li*

Laboratory of Photoelectron Imaging Technology and System of Ministry of Education, School of Optoelectronics, Beijing Institute of Technology, Beijing 100081, China

*Corresponding author: liyanqiu@bit.edu.cn

Received 5 January 2015; revised 3 February 2015; accepted 3 February 2015; posted 4 February 2015 (Doc. ID 231896); published 9 March 2015

The low source power is one of the major challenges that hinder the extreme ultraviolet lithography from high volume manufacturing. To alleviate the source development pressure, a high-efficiency illumination system with three mirrors is proposed, based on the authors' knowledge, for the first time. Free-form fly's eye is introduced into the system to get a qualified arc-shaped irradiance distribution on the reticle. A method integrated with a numerical method and optimization to design the free-form surface is given in detail. The transfer efficiency of the system is much higher than that of the four-mirror configuration employed in the EUV exposure platform. Compared with the previous high-efficiency illumination system with two mirrors, this configuration can ensure a good uniformity and will not increase the objective design difficulty or affect the image quality of the objective. Simulation result of the design with three mirrors shows the uniformity on the reticle is about 95.5%, and the energy efficiency is about 25.4%. It indicates that the system is effective in enhancing the efficiency and potential to promote the EUV lithography into high volume manufacturing.

OCIS codes: (220.4298) Nonimaging optics; (220.2945) Illumination design; (340.7480) X-rays, soft x-rays, extreme ultraviolet (EUV); (220.3740) Lithography.

http://dx.doi.org/10.1364/AO.54.002091

1. Introduction

Extreme ultraviolet (EUV) lithography is one of the candidates for the 22-nm half-pitch and below [1]. The EUV exposure system consists of three parts: the source subsystem, the illumination system, and the projection objective. To achieve cost-effectiveness in EUV lithography and enable high volume manufacturing, the low output of the source subsystem is one of the major challenges [2]. To deal with this problem, several illumination systems with higher energy transfer efficiency have been proposed in the past several years.

The illumination system employed in the EUV exposure platform is usually made up of two subsystems. The first one is the fly's eye to get an arc-shaped uniform irradiance including the field facet mirror on the field plate, and the pupil facet mirror on the pupil plate. Another one is two relay mirrors to realize the conjugate relationship between the pupil facet mirror and the entrance pupil of the objective. The field facet mirror includes a plurality of reflective elements named field facets. Each of the elements is arc in cross section. The pupil facet mirror includes a plurality of reflective elements named pupil facets. To increase the transfer efficiency of the system, Singer and Ulrich introduced a new field facet mirror into the four-mirror system [3]. The field facets are configured of different dimensions and aspect ratio so that a better covering of the illuminated

1559-128X/15/082091-07$15.00/0

area by the field facets can be achieved. In this way, more light is captured into the system, and thus a high efficiency results. Despite this, the energy utilization of the system can be increased by about only 10%.

Goldstein established the illumination system with only two mirrors [4]. The system used a free-form facet array followed by a single relay mirror. An arc-shaped irradiance with uniformity of 96.6% can be achieved by the facet array. The point of his work is to decrease the number of reflections even if it increases the complexity of the fly's eye. Thus, it is very difficult to fabricate the design.

Another new two-mirror configuration was presented by Singer and Martin [5]. The first one consists of thousands of different spherical facets located on a plate, and the second one is a normal-incidence imaging mirror to realize a feasible structure space for the source subsystem. Because the configuration employs critical configuration, a qualified uniformity on the reticle is hard to achieve.

Mann and Singer also proposed an illumination system with two mirrors [6]. Compared with the four-mirror system, no relay is employed in this configuration. The conjugate relationship between the pupil facets and the entrance pupil of the objective is accomplished by directly depositing the pupil plate on the plane overlapping with the entrance pupil. However, to avoid obstruction, the objective has to leave enough space for the pupil facets, which greatly increases the difficulty in the objective design. At the same time, the illumination system and the objective in this configuration have to be installed in the same vacuum chamber. In this way, the image performance of the objective would deteriorate significantly for the stray light in the illumination system. In a word, there are still some critical issues in the illumination systems with two or four mirrors discussed above.

In this contribution, a high-efficiency illumination system with three mirrors is proposed. The uniform irradiance on the reticle is ensured by employing Kohler configuration with fly's eye. Then, a relay mirror is used to image the pupil facet mirror to the entrance pupil of the objective. Free-form surface is introduced so that an arc-shaped irradiance can be achieved. A design method for the free-from surface integrated with a numerical method and optimization is given. As the system consists of only two

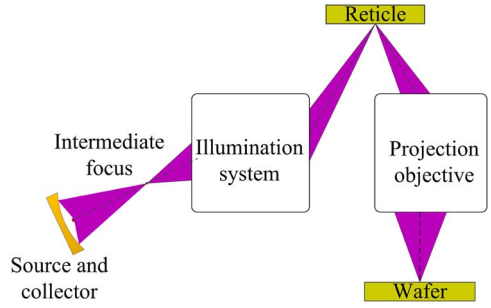

Fig. 1. Typical sketch of a EUV exposure system.

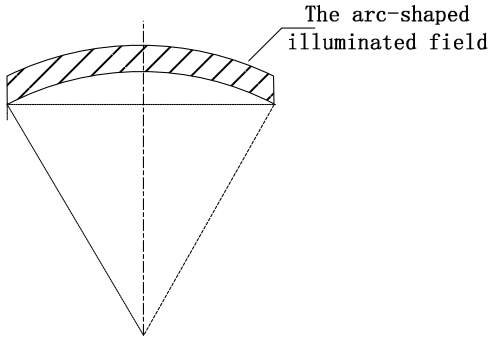

Fig. 2. Arc-shaped field on the reticle.

normal-incidence mirrors and one grazing-incidence mirror, the energy efficiency is much higher than the four-mirror system. At the same time, compared with the designs with two mirrors, this configuration can ensure a good uniformity and avoid bringing new challenges to the objective design. It can be utilized as a promising solution to the source power issues and further promote the EUV lithography into high volume manufacturing.

2. Configuration of the Three-Mirror Illumination System

Figure 1 shows the typical sketch of EUV exposure system. As one of the key components, the illumination system should meet two main requirements. The first one is to achieve a uniform illumination across the arc-shaped field on the reticle shown in Fig. 2. The other is that the exit pupil of the illumination system should coincide with the entrance pupil of the objective and provide different illumination modes for the exposure tool. Because the requirement for the irradiance uniformity on the reticle is very high, the illumination system always employs Kohler configuration.

Figure 3 shows the illumination system with three mirrors. The first two mirrors works as the fly's eye, and the last one is used as an imaging element. Beam emitted from the intermediate focus (IF) strikes on the field facet mirror. Hundreds of field facets divide the beam into different channels and direct them to the pupil facets. Then, the image of each field facet will be formed by the relative pupil facet and overlaps each other at a specific position. Downstream, a conic mirror is employed as a relay. The conjugate relationship between the pupil facets and entrance pupil of the objective is realized by the conic relay

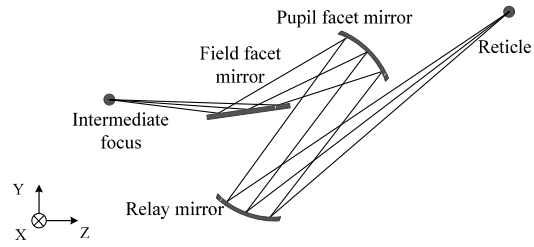

Fig. 3. High-efficiency illumination system with three mirrors.

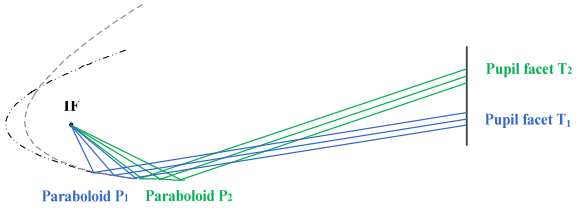

Fig. 4. Rule to generate the paraboloids.

mirror. At the same time, the superimposed image of the field facets is imaged to the reticle plane.

Because the field facet mirror operates at a grazing-incidence angle, it is difficult to get an arc-shaped irradiance distribution with the conventional field facet of arc cross section. To deal with this problem, a free-form surface is used to construct each of the pupil facets. At the same time, each field facet is set to be a paraboloid. It helps simplify the design of the pupil facet greatly. All the paraboloids share the IF as the common focus. For each paraboloid, the line determined by the IF and relative pupil facet is the symmetry axis. Figure 4 illustrates the rule to generate the paraboloids. The cross section of each field facet is a rectangle. To avoid obstruction, the field facet at the edge of the field facet plate has a smaller width than that of the facets in the center of the plate. When the design of the fly's eye is finished, a conic mirror can be deposited to realize the conjugate relationships.

Compared with the two-mirror illumination systems, there are two main advantages of this configuration. First, three mirrors can provide enough freedom degrees for the system to employ Kohler configuration with fly's eye to achieve a qualified uniformity on the reticle. At the same time, the third mirror can be utilized as a relay to realize the conjugate relationship between the pupil facets and the entrance pupil of the objective. In this way, the problems in the two-mirror systems discussed above can be avoided. Second, with a grazing-incidence surface, the three-mirror illumination system is also capable to make sure the source and the mask located in a different side of the illumination system, which is always realized based on an even number of mirrors in previous illumination system.

3. Method to Design the Free-Form Pupil Facet

The coordinate of each component in the illumination system can be computed with the reverse ray-trace method [7]. In this section, we will focus on the design of the free-form pupil facets. Because each of the pupil facets functions in a similar way, we just introduce the design of one pupil facet.

A few design algorithms to calculate free-form surfaces that generate irradiance distributions have been proposed [8–12]. Presently, designing a smooth optical freeform lens is still a challenge of nonimaging optics [13,14]. Here, we employ a design method integrated with a numerical method and an optimization to achieve a smooth freeform pupil facet. The numerical method is used to create a starting design,

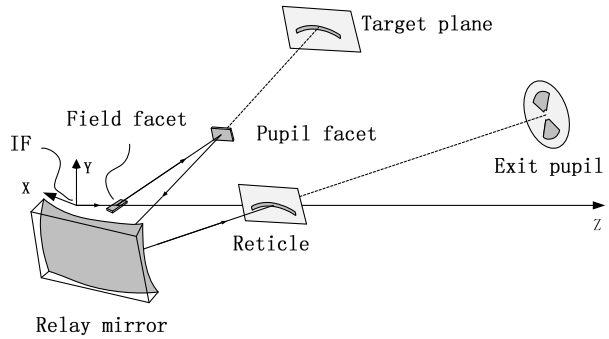

Fig. 5. Location of the target plane.

while the optimization method aims to improve the shape of the illumination area and enhance irradiance uniformity.

We adopt the numerical method presented by Ding *et al.* [12] to get the starting design. For clarification, we set up a XYZ coordinate system for the system shown in Fig. 3 based on the right-hand rule. The Y axis runs upward, and the Z axis runs to the right. A set of partial differential equations can be obtained as follows:

$$\begin{cases} z_x = f_1(x, y, z, t_x, t_y) \\ z_y = f_2(x, y, z, t_x, t_y) \end{cases}, \tag{1}$$

where (x, y, z) is the coordinate of point P on the free-form surface, and (t_x, t_y) is the coordinate of point T on the target plane which is conjugate with the reticle. The terms z_x and z_y are first-order partial derivatives of z, respectively. Figure 5 shows the location of the target plane. Coordinate of the target plane is $(0, \mathrm{l}, z_{\mathrm{target}})$, and it remains the same for the design of each free-form pupil facet.

To solve Eq. (1), specific coordinate relationships between point P and its corresponding point T should be established.

The rays form a parallelogram on the free-form surface. We use (x_A, y_A), (x_B, y_B), (x_A, y_C), and (x_B, y_D), respectively, to denote the coordinate of the four vertexes in the parallelogram. Then, the rays impinge on the target plane with an arc-shaped illuminated field. The arc is made up by two concentric circles. r_{out} is the radius of the outer circle, and r_{in} is the radius of the inner circle. θ_0 represents the half-angular range extended by the arc. Figure 6 shows

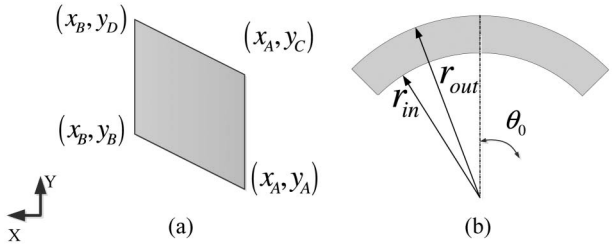

Fig. 6. Illuminated area: (a) on the free-form surface; (b) on the target plane.

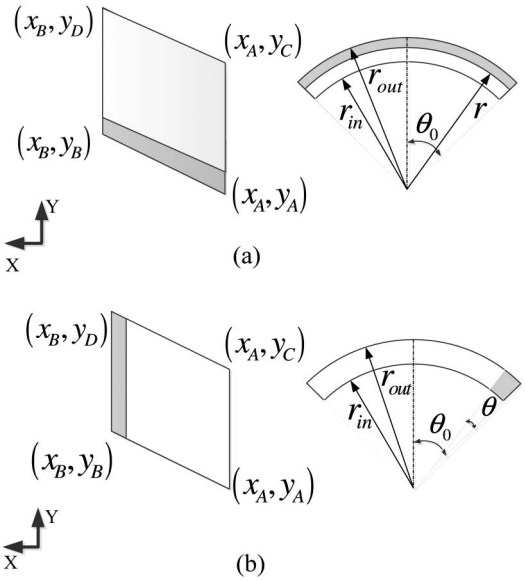

Fig. 7. Mapping relationship of the points on the two planes: (a) in X direction; (b) in Y direction.

the illuminated area on the free-form surface and the target plane, respectively.

On one hand, the power on the free-form surface can be expressed by Eq. (2):

$$\text{Power}_{\text{free-form}} = I(x_B - x_A)(y_C - y_A), \tag{2}$$

where I is the irradiance on the free-form surface. Because the cross section of each field facet is small, I is assumed to be a constant.

On the other hand, the power on the target plane can be formulated by Eq. (3):

$$\text{Power}_{\text{target}} = \int_{r_{\text{in}}}^{r_{\text{out}}} 2E\theta_0 r\mathrm{d}r, \tag{3}$$

where E is the radiant intensity on the target plane.

According to light transmission energy conservation condition, the power on the free-from surface is equal to that of the target plane. Thus, we can achieve:

$$E = \frac{I(x_B - x_A)(y_C - y_A)}{\theta_0(r_{\text{out}}^2 - r_{\text{in}}^2)}. \tag{4}$$

Figure 7 shows the mapping relationship of the points on the two planes in X and Y directions, respectively.

In Fig. 7(a), rays within the parallelogram depicted dark will be reflected, and form a uniform arc irradiance distribution on the target plane. The outer radius is r_{out}, and the inner radius is r. Then, based on the light transmission energy conservation condition, we get:

$$\int_{y_m}^{y} I(x_B - x_A)\mathrm{d}y = \int_{r}^{r_{\text{out}}} 2E\theta_0 r\mathrm{d}r. \tag{5}$$

In Eq. (5), y_m is defined as following: there is a point P′ on the base of the parallelogram; the x coordinate of point P′ is the same as that of point P; the y coordinate of P′ is defined as y_m. (r, θ) is the polar coordinate of point T.

In Fig. 7(b), rays within the parallelogram depicted dark will be reflected and form a uniform fan-shaped irradiance distribution with dark color on the target plane. The outer radius is r_{out}, and the inner radius is r_{in}. The angular range extended by the fan-shaped area is θ. Then, based on the light transmission energy conservation condition, we get:

$$\int_{x_A}^{x} I(y_C - y_A)\mathrm{d}x = \int_{r_{\text{in}}}^{r_{\text{out}}} E\left(\theta - \frac{\pi}{2} + \theta_0\right) r\mathrm{d}r. \tag{6}$$

By substituting Eq. (4) into Eqs. (5) and (6), we get:

$$\theta = \frac{2(x - x_A)}{x_B - x_A} \times \theta + \frac{\pi}{2} - \theta_0, \tag{7}$$

$$r = \sqrt{r_{\text{out}}^2 - \frac{y - y_m}{y_C - y_A} \times (r_{\text{out}}^2 - r_{\text{in}}^2)}. \tag{8}$$

At the same time, the coordinate of point T can be expressed as

$$\begin{cases} tx = r\cos\theta \\ ty = r\sin\theta + l - \frac{r_{\text{in}} + r_{\text{out}}}{2} \end{cases}. \tag{9}$$

Equations (7)–(9) depict the relationship between the points on the free-form surface and the points on the target plane. We can use them to solve Eq. (1) with appropriate numerical methods. A set of discrete data points are obtained, and the starting design can be generated by interpolating these points with a smooth spline surface.

After the process to get the starting design, the free-form surface needs to be optimized to get a qualified performance. The discrete points of the free-form surface are input in LightTools (optical research association), and we establish the surface as spline patch. Points are evenly distributed over the free-form surface in LightTools. To start the optimization, variables should be carefully selected by taking into account both search efficiency and the performance of the reflector. For example, we choose 41×6 variables in $X \times Y$ direction in the following design example. Then, the ray-based merit functions embedded in LightTools is chosen. It is constructed with the position deviation on the target plane for each ray:

$$\text{MF} = \sum_{i=1}^{N} \omega_i \sqrt{(x_i - x_{ti})^2 + (y_i - y_{ti})^2}, \tag{10}$$

where N is the number of rays, (x_i, y_i) is the actual position of the i-th ray on the reticle, (x_{ii}, y_{ii}) is the prescribed position of the i-th ray on the reticle, and ω_i is the weight.

Table 1. Parameters of the Objective

Item	Exposure Field (mm)	Reduction	NA	Entrance Pupil Distance (mm)
Objective	104×6 $r_{\text{in\_reticle}} = 135$ $r_{\text{out\_reticle}} = 141$	4	0.3	1375.539

Table 2. Parameters of the Fly's Eye Element

Element	Parameters		
	Length (mm)	Width (mm)	Size of Full Array (mm)
Field facet	4	3–4	$a = 31.46$, $b = 194.54$
Pupil facet	3.56–4.04	0.59–1.72	$D_{\text{pf}} = 87.90$

4. Design of the Three-Mirror Illumination System

An illumination system with the configuration described above for a given projection objective was designed in this section. Parameters of the objective are listed in Table 1. NA is the numerical aperture of the objective in image space. $r_{\text{out\_reticle}}$ is the radius of the outer circle of the arc on the reticle, and $r_{\text{in\_reticle}}$ is the radius of the inner circle of the arc on the reticle.

As the dimension of Laser Produced Plasma is about 20 μm [15], which is small enough compared with the system, we employ a point source at the intermediate focus for the following simulation. There are 196 field facets in the illumination system. Figure 8 shows the arrangements of field facets. Parameters "a" and "b" show the size of the full array. All of the field facets are deposited within an elliptic area. Figure 9 shows the arrangements of the pupil facets under different illumination modes. Only the ones depicted by dark color are illuminated in each mode. The parameters of the fly's eye element are listed in Table 2, where D_{pf} represents the diameter of the pupil facet mirror.

Figure 10 shows the structure of illumination system in LightTools. The track length of the system is about 2269.40 mm. When the system is set to realize a different illumination mode, the new fly's eye can be achieved based on the corresponding arrangement of the pupil facets and the design method described above. In the following, the illumination system under dipole illumination mode will be taken as an example to evaluation. Performance of the illumination system is evaluated in terms of efficiency and uniformity delivered to the reticle plane.

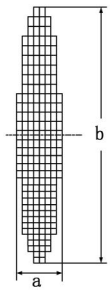

Fig. 8. Arrangement of field facets.

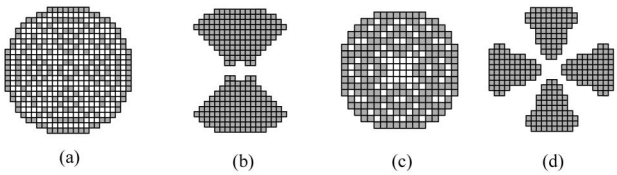

Fig. 9. Arrangement of pupil facets under different illumination modes: (a) conventional mode; (b) 90-degree dipole mode; (c) annular mode; (d) 45-degree quadrupole mode.

A. Efficiency of the System

The total luminous flux delivered to the reticle is a primary concern for illumination system. In this system, the light efficiency is determined by:

$$\text{Eff} = \eta_{\text{FF collecting}} \times \eta_{\text{FF}} \times \eta_{\text{PF}} \times \eta_{\text{RELAY}} \times \eta_{\text{reticle}}, \quad (11)$$

where η_{FF}, η_{PF} and η_{RELAY} are the reflectivity of the field facet mirror, the pupil facet mirror, and the relay mirror, respectively. Here, the reflectivity of multilayer-coated surfaces for normal-incidence surface and grazing-incidence surface is set to be 70% and 90%, respectively [16]. $\eta_{\text{FF collecting}}$ is the efficiency of all the field facets to collect the incident beam. η_{reticle} represents the ratio of the light irradiance within the standard arc-shaped field to the total irradiance on the reticle. $\eta_{\text{FF collecting}}$ and η_{reticle} strongly depend on the key parameters such as the dimension of each field facet and the performance of the pupil facets. To get the value of $\eta_{\text{FF collecting}}$ and η_{reticle}, we start the ray-trace in LightTools. For the system with the facets shown in Figs. 6 and 7, $\eta_{\text{FF collecting}}$ and η_{reticle} are estimated to be 64% and 90%, respectively. Therefore, the efficiency of the illumination system can be calculated as

$$\text{Eff} = 64\% \times 90\% \times 70\% \times 70\% \times 90\% = 25.4\%. \quad (12)$$

Comparatively, we can calculate the efficiency of the four-mirror illumination system. Based on the ratio of the field facets' size to that of the whole field

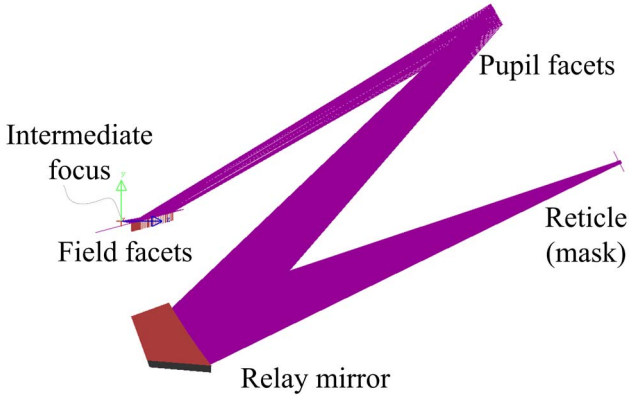

Fig. 10. Configuration of the high-efficiency illumination system.

facet plate illuminated, $\eta_{\mathrm{FF_{collecting}}}$ is set to be 85% approximately. Then, the efficiency is given by:

$$\mathrm{Eff}' = 85\% \times 70\% \times 70\% \times 70\% \times 70\% \times 90\% = 18.4\%. \quad (13)$$

From Eqs. (12) and (13) we can see that the efficiency is increased by nearly 38.0%. This shows the novel configuration in the paper is highly efficient.

B. Irradiance Uniformity of the System

The irradiance uniformity of the illumination system is calculated within the arc-shaped ring on the reticle:

$$U = \left(1 - \frac{E_{\max} - E_{\min}}{E_{\max} + E_{\min}}\right) \times 100\%, \quad (14)$$

where $E_{\max}$ and $E_{\min}$, respectively, presents the maximum and minimum line integral in scanning direction over the irradiance distribution. With the LightTools ray-tracing program, 200,000,000 rays are created at the IF and then traced nonsequentially. Figure 11 shows the irradiance distribution on the reticle. The uniformity is approximately 95.5%.

Because the grazing incidence element is usually very sensitive to the alignment, the alignment sensitivity of the grazing incidence elements is roughly analyzed. The surface rotation angle, X, Y, and Z coordinate are taken into account.

First, the sensitivity of single field facet is analyzed. One of the field facets is selected. A local coordinate system is defined: the origin is located at the center of the field facet; the x, y, and z axes in the local coordinate system are, respectively, parallel to the X, Y, and Z axes in the global coordinate system. Then, the field facet is moved along $+x$, $+y$, and $+z$ directions for 0.3 mm, respectively. Monte Carlo ray-tracing is implemented to evaluate the uniformity of the illumination systems, respectively. Next, the initial selected field facet located at the origin in local coordinate system is rotated round the x, y, and z axes for 0.3 degree, respectively. Uniformity of these three illumination systems is evaluated in the same way as described above. This process is carried out for each of the field facets. The local coordinate system is different for each field facet and set up in the same way described above.

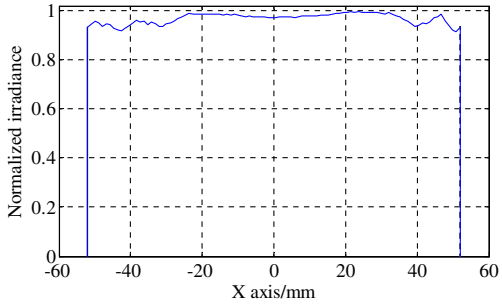

Fig. 11. Normalized irradiance distribution on the reticle.

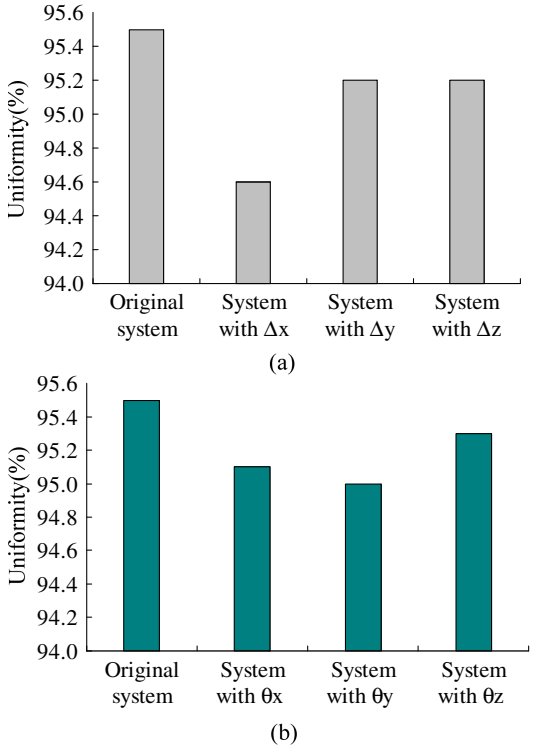

Fig. 12. Uniformity of the illumination system when one of the sensitive field facet: (a) moves along different axis; (b) rotates round different axis.

Results show the illumination system is comparatively more sensitive to the position and rotation angle of the field facets which receive more energy from the source. We select one of these sensitive field facet and evaluate the illumination system when the facet changes coordinate and rotation angle one by one. Figure 12 shows the uniformity of the system under different conditions. Δx, Δy, and Δz, respectively, represent the x, y, and z coordinate variations of the field facet. θ_x, θ_y, and θ_z, respectively, represent the rotation angle round x, y, and z axes. It seems that the system is a little more sensitive to the movement of single field facet along the x coordinate.

At the same time, the sensitivity analysis is also carried out when all the field facets are treated as a group in LightTools. The movement of the group along $+x$, $+y$, and $+z$ axis is 8 μm, and the rotation angle is 0.005 degree. Figure 13 shows the uniformity of the illumination system when the group changes coordinate and rotation angle, respectively. Results show the system is very sensitive to the movement along the x coordinate and θ_y.

The preliminary explanation for the alignment sensitivity of single element and the group is given: When the x coordinate or θ_y changes, the arc-shaped irradiance would move in the direction perpendicular to the scanning direction of the lithography tool. This would obviously deteriorate the uniformity of the irradiance on the reticle. Therefore, the x

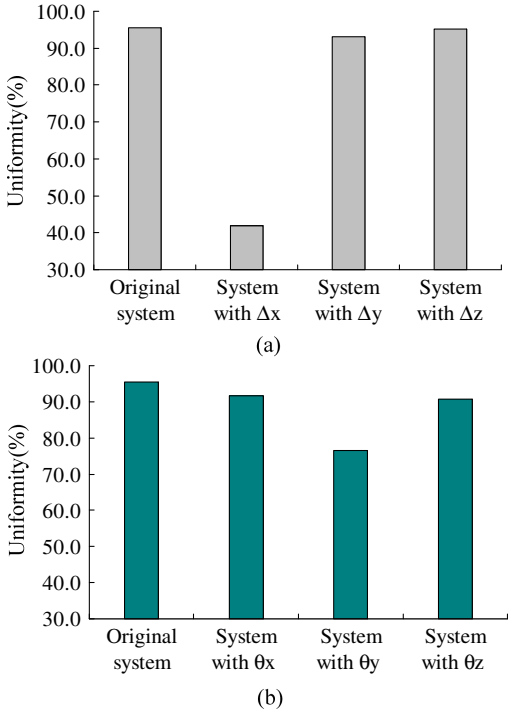

Fig. 13. Uniformity of the illumination system when the group: (a) moves along different axis; (b) rotates round different axis.

coordinate and θ_y of single element and the group should be controlled strictly during the alignment.

5. Conclusion

In this paper, we propose a high-efficiency illumination system with three mirrors for EUV lithography. Free-form surfaces are introduced to ensure a qualified irradiance distribution. The design method of the free-form surface is described in detail. The transfer efficiency of the system is much higher than that of the four-mirror configuration. Compared with the two-mirror illumination systems, the proposed system can ensure a good uniformity, and bring no new requirements to the objective design at the same time. The design results show that the system could offer a high transfer efficiency of about 25.4% and an irradiance uniformity of about 95.5%. It demonstrates the proposed illumination system is superior to the existing systems and is potential to promote the EUV lithography into high volume manufacturing.

We thank the financial support by National Science and Technology Major Project (2012ZX02702001-002).

References

1. International Technology Roadmap for Semiconductors (2013).
2. R. Peeters, S. Lok, J. Mallam, M. V. Noordenbrug, N. H. Arned, P. Kuerz, M. Lowisch, E. V. Setten, G. Schiffelers, A. Pirati, J. Stoeldraijer, D. Brandt, N. Farrar, I. Fomenkov, H. Boom, H. Meiling, and R. Kool, "EUV lithography: NXE plateform performance overview," Proc. SPIE **9048**, 904811 (2014).
3. W. Singer, W. Ulrich, and M. Antoni, "Illumination system with raster elements of different sizes," U.S. Patent 7,400,699 B2 (July 15, 2008).
4. M. Goldstein and V. Bakshi, "Optical design for affordable EUV lithography," (2007). http://www.sematech.org/meetings/archives/litho/8059/pres/OP-02-Goldstein.pdf.
5. W. Singer and M. Antoni, "Optical element for an illumination system," U.S. Patent 20,060,132,747 (June 22, 2006).
6. H. J. Mann and W. Singer, "Projection objective and projection exposure apparatus with negative back focus of the entry pupil," U.S. Patent 7,869,138 (Jan. 11, 2011).
7. Q. Mei, Y. Li, and F. Liu, "A Reverse design method for EUV lithography illumination system," Proc. SPIE **8679**, 867923 (2013).
8. C. Canavesi, W. J. Cassarly, and J. P. Rolland, "Observation on the linear programming formulation of the single reflector design problem," Opt. Express **20**, 4050–4055 (2012).
9. W. Tai and R. Schwarte, "Design of an aspherical lens to generate a homogenous irradiance for three-dimensional sensors with a light-emitting diode source," Appl. Opt. **39**, 5801–5805 (2000).
10. H. Ries and J. Muschaweck, "Tailored freeform optical surfaces," J. Opt. Soc. Am. A **19**, 590–595 (2002).
11. J. C. Minano and J. C. Gonzalez, "New method of design of nonimaging concentrators," Appl. Opt. **31**, 3051–3060 (1992).
12. Y. Ding, X. Liu, Z. R. Zheng, and P. F. Gu, "Freeform LED lens for uniform illumination," Opt. Express **16**, 12958–12966 (2008).
13. R. Wu, Z. Zheng, H. Li, and X. Liu, "Optimization design of irradiance array for LED uniform rectangular illumination," Appl. Opt. **51**, 2257–2263 (2012).
14. C. R. Prins, J. Boonkkamp, J. V. Roosmalen, W. L. Ijzerman, and T. W. Tukker, "A Monge-ampere-solver for free-form reflector design," Siam J. Sci. Comput. **36**, B640–B660 (2014).
15. A. Hassanein and T. Sizyuk, "Advances in computer simulations of LPP source for EUV Lithography," Proc. SPIE **8679**, 86790B (2013).
16. S. H. Lee and M. Goldstein, "Broad-angle multilayer mirror design," U.S. Patent 7,522,335 (Apr. 21, 2009).